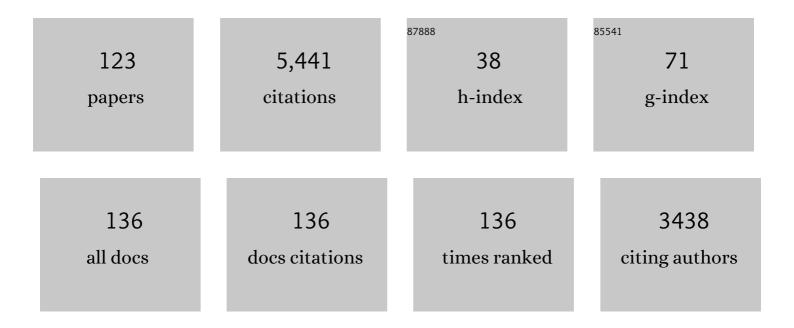
## Roberto Orosei

List of Publications by Year in descending order

Source: https://exaly.com/author-pdf/7792235/publications.pdf Version: 2024-02-01



#	Article	IF	CITATIONS
1	Radar evidence of subglacial liquid water on Mars. Science, 2018, 361, 490-493.	12.6	346
2	Subsurface Radar Sounding of the South Polar Layered Deposits of Mars. Science, 2007, 316, 92-95.	12.6	330
3	Radar Soundings of the Subsurface of Mars. Science, 2005, 310, 1925-1928.	12.6	327
4	The organic-rich surface of comet 67P/Churyumov-Gerasimenko as seen by VIRTIS/Rosetta. Science, 2015, 347, aaa0628.	12.6	293
5	SHARAD sounding radar on the Mars Reconnaissance Orbiter. Journal of Geophysical Research, 2007, 112, .	3.3	273
6	Mars North Polar Deposits: Stratigraphy, Age, and Geodynamical Response. Science, 2008, 320, 1182-1185.	12.6	271
7	The diurnal cycle of water ice on comet 67P/Churyumov–Gerasimenko. Nature, 2015, 525, 500-503.	27.8	199
8	Cryovolcanic features on Titan's surface as revealed by the Cassini Titan Radar Mapper. Icarus, 2007, 186, 395-412.	2.5	191
9	SHARAD: The MRO 2005 shallow radar. Planetary and Space Science, 2004, 52, 157-166.	1.7	153
10	Radar Sounding of the Medusae Fossae Formation Mars: Equatorial Ice or Dry, Low-Density Deposits?. Science, 2007, 318, 1125-1128.	12.6	143
11	The Mars express MARSIS sounder instrument. Planetary and Space Science, 2009, 57, 1975-1986.	1.7	134
12	Multiple subglacial water bodies below the south pole of Mars unveiled by new MARSIS data. Nature Astronomy, 2021, 5, 63-70.	10.1	127
13	Performance and surface scattering models for the Mars Advanced Radar for Subsurface and Ionosphere Sounding (MARSIS). Planetary and Space Science, 2004, 52, 149-156.	1.7	125
14	Exposed water ice on the nucleus of comet 67P/Churyumov–Gerasimenko. Nature, 2016, 529, 368-372.	27.8	104
15	Shallow radar (SHARAD) sounding observations of the Medusae Fossae Formation, Mars. Icarus, 2009, 199, 295-302.	2.5	102
16	JIRAM, the Jovian Infrared Auroral Mapper. Space Science Reviews, 2017, 213, 393-446.	8.1	91
17	Accumulation and Erosion of Mars' South Polar Layered Deposits. Science, 2007, 317, 1715-1718.	12.6	84
18	Virtis : an imaging spectrometer for the rosetta mission. Planetary and Space Science, 1998, 46, 1291-1304.	1.7	72

#	Article	IF	CITATIONS
19	Mars Advanced Radar for Subsurface and Ionospheric Sounding (MARSIS) after nine years of operation: A summary. Planetary and Space Science, 2015, 112, 98-114.	1.7	66
20	Titan's diverse landscapes as evidenced by Cassini RADAR's third and fourth looks at Titan. Icarus, 2008, 195, 415-433.	2.5	65
21	SHARAD radar sounding of the Vastitas Borealis Formation in Amazonis Planitia. Journal of Geophysical Research, 2008, 113, .	3.3	63
22	Self-affine behavior of Martian topography at kilometer scale from Mars Orbiter Laser Altimeter data. Journal of Geophysical Research, 2003, 108, .	3.3	61
23	Seasonal exposure of carbon dioxide ice on the nucleus of comet 67P/Churyumov-Gerasimenko. Science, 2016, 354, 1563-1566.	12.6	61
24	The Main Belt Comets and ice in the Solar System. Astronomy and Astrophysics Review, 2017, 25, 1.	25.5	60
25	RIME: Radar for Icy Moon Exploration. , 2013, , .		57
26	Mars Express investigations of Phobos and Deimos. Planetary and Space Science, 2014, 102, 18-34.	1.7	54
27	Direct observations of asteroid interior and regolith structure: Science measurement requirements. Advances in Space Research, 2018, 62, 2141-2162.	2.6	54
28	Quantitative analysis of Mars surface radar reflectivity at 20MHz. Icarus, 2012, 220, 84-99.	2.5	52
29	Dielectric properties of Jovian satellite ice analogs for subsurface radar exploration: A review. Reviews of Geophysics, 2015, 53, 593-641.	23.0	52
30	Subsurface Radar Sounding of the Jovian Moon Ganymede. Proceedings of the IEEE, 2011, 99, 837-857.	21.3	49
31	Mars ionosphere total electron content analysis from MARSIS subsurface data. Icarus, 2013, 223, 423-437.	2.5	49
32	Observations of Vertical Reflections from the Topside Martian Ionosphere. Space Science Reviews, 2007, 126, 373-388.	8.1	47
33	Annual variations in the Martian bow shock location as observed by the Mars Express mission. Journal of Geophysical Research: Space Physics, 2016, 121, 11,474.	2.4	44
34	Transition Elements between Comets and Asteroids. Icarus, 1997, 129, 317-336.	2.5	43
35	Small edifice features in Chryse Planitia, Mars: Assessment of a mud volcano hypothesis. Icarus, 2016, 268, 56-75.	2.5	43
36	A P/Wirtanen evolution model. Planetary and Space Science, 1996, 44, 987-1000.	1.7	41

#	Article	IF	CITATIONS
37	Chiron Activity and Thermal Evolution. Astronomical Journal, 2000, 119, 3112-3118.	4.7	41
38	Climate-driven deposition of water ice and the formation of mounds in craters in Mars' north polar region. Icarus, 2012, 220, 174-193.	2.5	41
39	Solar cycle variations in the ionosphere of Mars as seen by multiple Mars Express data sets. Journal of Geophysical Research: Space Physics, 2016, 121, 2547-2568.	2.4	40
40	Transition Elements between Comets and Asteroids. Icarus, 1997, 129, 337-347.	2.5	38
41	Models of P/Wirtanen nucleus: active regions versus non-active regions. Planetary and Space Science, 1999, 47, 855-872.	1.7	36
42	New 3D thermal evolution model for icy bodies application to trans-Neptunian objects. Astronomy and Astrophysics, 2011, 529, A71.	5.1	34
43	Titan as Revealed by the Cassini Radar. Space Science Reviews, 2019, 215, 1.	8.1	34
44	Thermal evolution and differentiation of a short-period comet. Planetary and Space Science, 1993, 41, 409-427.	1.7	33
45	Vertical sheets of dense plasma in the topside Martian ionosphere. Journal of Geophysical Research, 2007, 112, .	3.3	33
46	Ground penetrating radar investigations to study active faults in the Norcia Basin (central Italy). Journal of Applied Geophysics, 2010, 72, 39-45.	2.1	33
47	Total electron content in the Martian atmosphere: A critical assessment of the Mars Express MARSIS data sets. Journal of Geophysical Research: Space Physics, 2015, 120, 2166-2182.	2.4	32
48	Jupiter ICY moon explorer (JUICE): Advances in the design of the radar for Icy Moons (RIME). , 2015, , .		29
49	An incoherent simulator for the SHARAD experiment. , 2008, , .		27
50	The Castalia mission to Main Belt Comet 133P/Elst-Pizarro. Advances in Space Research, 2018, 62, 1947-1976.	2.6	27
51	Origin of the Extended Mars Radar Blackout of September 2017. Journal of Geophysical Research: Space Physics, 2019, 124, 4556-4568.	2.4	27
52	The exploration of Titan with an orbiter and a lake probe. Planetary and Space Science, 2014, 104, 78-92.	1.7	26
53	Explorer of Enceladus and Titan (E2T): Investigating ocean worlds' evolution and habitability in the solar system. Planetary and Space Science, 2018, 155, 73-90.	1.7	26
54	Thermal Evolution of the Centaur Object 5145 Pholus. Astronomical Journal, 2000, 120, 1571-1578.	4.7	24

#	Article	IF	CITATIONS
55	Dielectric constant estimation of the uppermost Basal Unit layer in the martian Boreales Scopuli region. Icarus, 2012, 219, 458-467.	2.5	23
56	Results from the comet nucleus model team at the international space science institute, Bern, Switzerland. Advances in Space Research, 1999, 23, 1283-1298.	2.6	20
57	MUSES: multi-sensor soil electromagnetic sounding. Planetary and Space Science, 2004, 52, 67-78.	1.7	20
58	Permittivity estimation over Mars by using SHARAD data: the Cerberus Palus area. Journal of Geophysical Research, 2012, 117, .	3.3	20
59	Numerically improved thermochemical evolution models of comet nuclei. Planetary and Space Science, 1999, 47, 839-853.	1.7	19
60	Sounding the subsurface of Athabasca Valles using MARSIS radar data: Exploring the volcanic and fluvial hypotheses for the origin of the rafted plate terrain. Journal of Geophysical Research, 2009, 114, .	3.3	19
61	Permittivity estimation of layers beneath the northern polar layered deposits, Mars. Geophysical Research Letters, 2010, 37, .	4.0	18
62	Global permittivity mapping of the Martian surface from SHARAD. Earth and Planetary Science Letters, 2017, 462, 55-65.	4.4	18
63	JIRAM, the Image Spectrometer in the Near Infrared on Board the Juno Mission to Jupiter. Astrobiology, 2008, 8, 613-622.	3.0	17
64	Radar Signal Propagation and Detection Through Ice. Space Science Reviews, 2010, 153, 249-271.	8.1	17
65	Radar Signal Penetration and Horizons Detection on Europa Through Numerical Simulations. IEEE Journal of Selected Topics in Applied Earth Observations and Remote Sensing, 2017, 10, 118-129.	4.9	17
66	The Global Search for Liquid Water on Mars from Orbit: Current and Future Perspectives. Life, 2020, 10, 120.	2.4	16
67	The Mars Advanced Radar for Subsurface and Ionosphere Sounding (MARSIS): concept and performance. , 0, , .		15
68	Ionospheric corrections of MARSIS subsurface sounding signals with filters including collision frequency. Planetary and Space Science, 2009, 57, 393-403.	1.7	15
69	Assessing the role of clay and salts on the origin of MARSIS basal bright reflections. Earth and Planetary Science Letters, 2022, 579, 117370.	4.4	15
70	A working environment for digital planetary data processing and mapping using ISIS and GRASS GIS. Planetary and Space Science, 2011, 59, 1265-1272.	1.7	14
71	Improved estimation of Mars ionosphere total electron content. Icarus, 2018, 299, 396-410.	2.5	14
72	Removal of atmospheric features in near infrared spectra by means of principal component analysis and target transformation on Mars: I. Method. Icarus, 2015, 253, 51-65.	2.5	13

#	Article	IF	CITATIONS
73	The Impact of Energetic Particles on the Martian Ionosphere During a Full Solar Cycle of Radar Observations: Radar Blackouts. Journal of Geophysical Research: Space Physics, 2022, 127, .	2.4	13
74	Radar sounding of Lucus Planum, Mars, by MARSIS. Journal of Geophysical Research E: Planets, 2017, 122, 1405-1418.	3.6	12
75	Collision-induced thermal evolution of a comet nucleus in the Edgeworth-Kuiper Belt. Advances in Space Research, 2001, 28, 1563-1569.	2.6	11
76	Mars Advanced Radar for Subsurface and Ionosphere Sounding (MARSIS): subsurface performances evaluation. , 0, , .		11
77	MARSIS data inversion approach: Preliminary results. , 2008, , .		11
78	Topside of the martian ionosphere near the terminator: Variations with season and solar zenith angle and implications for the origin of the transient layers. Icarus, 2015, 251, 12-25.	2.5	10
79	CLUSIM: A Synthetic Aperture Radar Clutter Simulator for Planetary Exploration. Radio Science, 2017, 52, 1200-1213.	1.6	10
80	Comparison between MARSIS & amp;#x00026; SHARAD results. , 2007, , .		9
81	Periglacial geomorphology and landscape evolution of the Tempe Terra region, Mars. Geological Society Special Publication, 2011, 356, 43-67.	1.3	9
82	Mars' plasma system. Scientific potential of coordinated multipoint missions: "The next generation― Experimental Astronomy, 2022, 54, 641-676.	3.7	9
83	Martian underground water detection: Thermal model and simulations of radar signal propagation. Journal of Geophysical Research, 2003, 108, .	3.3	8
84	Correlations between VIMS and RADAR data over the surface of Titan: Implications for Titan's surface properties. Icarus, 2010, 208, 366-384.	2.5	8
85	Observations of Phobos by the Mars Express radar MARSIS: Description of the detection techniques and preliminary results. Advances in Space Research, 2017, 60, 2289-2302.	2.6	8
86	The banded terrain on northwestern Hellas Planitia: New observations and insights into its possible formation. Icarus, 2019, 321, 171-188.	2.5	8
87	Liquid Water Detection under the South Polar Layered Deposits of Mars—a Probabilistic Inversion Approach. Remote Sensing, 2019, 11, 2445.	4.0	7
88	The subsurface investigation by Mars Advanced Radar for Subsurface and Ionosphere Sounding (MARSIS). , 0, , .		6
89	Conditions for liquid or icy core existence in KBO objects: Numerical simulations for Orcus and Quaoar. Planetary and Space Science, 2014, 104, 147-155.	1.7	6
90	Resolution Enhancement and Interference Suppression for Planetary Radar Sounders. , 2018, , .		6

#	Article	IF	CITATIONS
91	Observations of Vertical Reflections from the Topside Martian Ionosphere. , 2007, , 373-388.		6
92	MARS-IRMA: in-situ infrared microscope analysis of Martian soil and rock samples Advances in Space Research, 2001, 28, 1219-1224.	2.6	5
93	MARSIS Data Inversion Approach. , 2007, , .		5
94	Saturn Satellites as Seen by Cassini Mission. Earth, Moon and Planets, 2009, 105, 289-310.	0.6	4
95	Ionosphere of Mars during the consecutive solar minima 23/24 and 24/25 as seen by MARSIS-Mars Express. Icarus, 2023, 393, 114616.	2.5	4
96	JIRAM, the Jovian Infrared Auroral Mapper. , 2014, , 271-324.		4
97	Numerical simulations of radar echoes rule out basal CO2 ice deposits at Ultimi Scopuli, Mars. Icarus, 2022, 386, 115163.	2.5	4
98	Varuna: Thermal evolution. Advances in Space Research, 2006, 38, 1946-1951.	2.6	3
99	SHARAD, a shallow radar sounder to investigate the red planet. , 2008, , .		3
100	Numerical computation of radar echoes measured by MARSIS during phobos flybys. , 2009, , .		3
101	A new method for determining the total electron content in Mars' ionosphere based on Mars Express MARSIS data. Planetary and Space Science, 2020, 182, 104812.	1.7	3
102	Exploration of Enceladus and Titan: investigating ocean worlds' evolution and habitability in the Saturn system. Experimental Astronomy, 2022, 54, 877-910.	3.7	3
103	Radar detection of subsurface features on Mars. Advances in Space Research, 2004, 33, 2263-2269.	2.6	2
104	The ISHTAR Mission: Probing the Internal Structure of NEOs. Highlights of Astronomy, 2005, 13, 738-742.	0.0	2
105	TITAN'S GROUND REFLECTANCE RETRIEVAL FROM CASSINI-VIMS DATA TAKEN DURING THE JULY 2ND, 2004 FLY-BY AT 2 AM UT. Earth, Moon and Planets, 2006, 96, 109-117.	0.6	2
106	Relationship of dayside main layer ionosphere height to local solar time on Mars and implications for solar wind interaction influence. Journal of Geophysical Research E: Planets, 2015, 120, 1427-1445.	3.6	2
107	Ducted electromagnetic waves in the Martian ionosphere detected by the Mars Advanced Radar for Subsurface and Ionosphere Sounding radar. Geophysical Research Letters, 2016, 43, 7381-7388.	4.0	2
108	A strategy for an accurate estimation of the basal permittivity in the Martian North Polar Layered Deposits. Geophysical Prospecting, 2017, 65, 891-900.	1.9	2

#	Article	IF	CITATIONS
109	Cassini radar : system concept and simulation results. Planetary and Space Science, 1998, 46, 1363-1374.	1.7	1
110	MARSIS Radar Data Interpretation to Characterize the Deeper Layers in the North Polar Cap on Mars. Advances in Astronautics Science and Technology, 2018, 1, 31-37.	0.8	1
111	Deep space orbit determination via Delta-DOR using VLBI antennas. CEAS Space Journal, 0, , 1.	2.3	1
112	Italian participation in the Mars exploration program. Advances in Space Research, 2001, 28, 1197-1202.	2.6	0
113	Subsurface Investigations by MARSIS in Mars Express Mission. , 2006, , .		0
114	Subsurface sounding in Northern hemisphere for Mars by MARSIS: Mars express mission. , 2008, , .		0
115	Exploring the Martian subsurface of Athabasca using MARSIS radar data: Testing the volcanic and fluvial hypotheses for the origin of the morphology. , 2009, , .		0
116	Radar subsurface sounding over the putative frozen sea in Cerberus Palus, Mars. , 2010, , .		0
117	Preliminary performance of Sub-Surface Radar for the EJSM/Laplace mission. , 2010, , .		0
118	A simple inversion model for the estimation of subsurface features of Mars poles. , 2010, , .		0
119	Probing the Hidden Geology of Isidis Planitia (Mars) with Impact Craters. Geosciences (Switzerland), 2015, 5, 30-44.	2.2	0
120	Volume Scattering Losses Evaluation for Radar Sounding of Jovian Icy Moons. , 2018, , .		0
121	Searching for Life on Mars: A Brief Summary. Springer Proceedings in Physics, 2021, , 115-122.	0.2	0
122	Radar Signal Propagation and Detection Through Ice. Space Sciences Series of ISSI, 2010, , 247-269.	0.0	0
123	Radar detection of subglacial water under the south polar cap of Mars: Where are we now?. , 2020, , .		0